B Geiger et al.

Study of the fast-ion distribution function in the TCV tokamak based on FIDA spectroscopy and the TRANSP code

Fast-ion transport study at TCV using FIDA spectroscopy and the TRANSP code

B. Geiger[1], A. N. Karpushov[2], B.P. Duval[2], C. Marini[2], O. Sauter[2], Y. Andrebe[2], D. Testa[2], M. Salewski[3], P.A. Schneider[1], the TCV Team[2] and the EUROfusion MST1 Team[4]

[1]Max-Planck-Institute for Plasma Physics, Boltzmannstr. 2, 85748 Garching, Germany
[2]Swiss Plasma Center, EPFL, Lausanne, Switzerland
[3]Technical University of Denmark, Dk-2800 Kgs. Lyngby, Denmark
[4]See appendix of H. Meyer et.al. (OV/P-12) Proc. 26th IAEA Fusion Energy Conf. 2016, Kyoto, Japan

Corresponding Author: benedikt.geiger@ipp.mpg.de

Abstract:

Experiments with 1 MW of neutral beam injection (NBI) have been performed at the TCV tokamak with high electron temperatures (3-5 keV) and low electron densities (about $1.6 \times 10^{19}/\text{m}^3$). Fast-Ion D-Alpha (FIDA) spectroscopy using two different optical systems observes high signals from the fast ions and is in qualitative agreement with TRANSP/NUBEAM simulations. In addition, clear effects on the loop voltage and plasma pressure are seen when switching on NBI. However, good quantitative agreement between the experimental data and TRANSP predictions is only found when considering additional fast-ion losses caused either by anomalous fast-ion transport or by charge-exchange. On the one hand, strong passive FIDA radiation indicates that the background neutral density is sufficient for non-negligible charge-exchange losses. On the other hand, high frequency modes are observed in magnetic data which could be responsible for an anomalous redistribution of fast ions.

Introduction The behavior of fast, suprathermal particles in high temperature plasmas must be understood in view of future fusion reactors. Fast ions will occur as results of the fusion process and can be generated in present day devices by neutral beam injection (NBI) or ion cyclotron resonance heating (ICRH). The fast particles heat the background plasma via collisions with ions and electrons and can, in case of an anisotropic fast-ion velocity space distribution, drive non-inductive currents. In the absence of plasma instabilities and modes, the fast-ion slowing down distribution is neoclassical and can be modeled by solving the Fokker Planck equation. This is of particular interest for present day fusion experiments because detailed information on the heating and current drive profiles is needed, e.g. for power balance analyses. Unfortunately, high temperature plasmas are not instability-free. Hence possible differences between actual fast-ion distribution functions and the neoclassical predictions must be studied. The TCV tokamak is well suited for fast ion transport studies since large fast ion densities can be generated by a
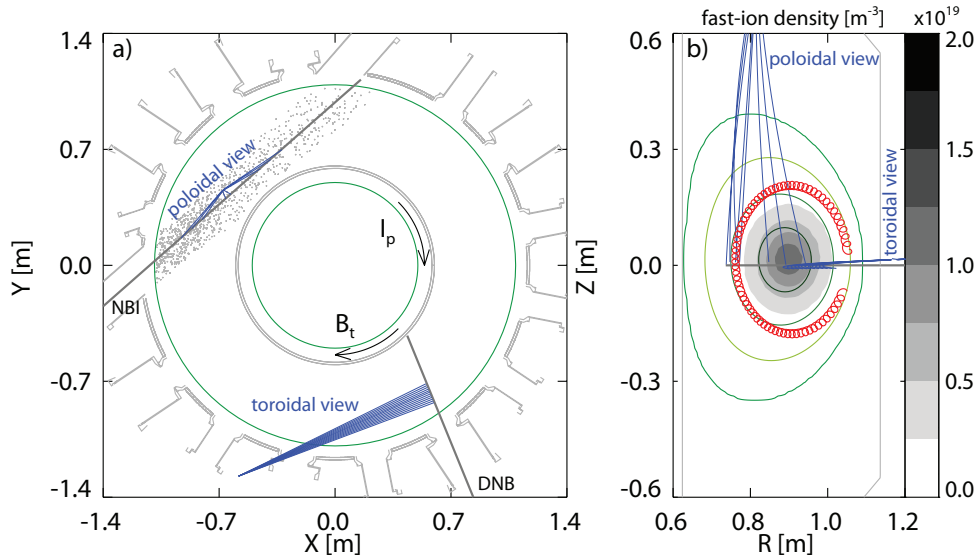
FIG. 1: *Top down (a) and poloidal (b) view on the TCV tokamak.*

newly installed 1 MW NBI[1]. In this paper, first the experimental setup at TCV is discussed followed by the presentation of experimental results using 1 MW of NBI. Finally, a short summary is provided.

Experimental Setup

The Tokamak à Configuration Variable (TCV) is a mid-size machine situated in Lausanne, Switzerland. The major and minor radii are about 0.88 m and 0.25 m, respectively. It uses carbon as main wall material and uses magnetic field strengths of up to 1.53 T and currents of up to 1 MA. During the experiments discussed here, up to 1.5 MW of electron cyclotron resonance heating (ECRH) were available from three launchers that were operated in second harmonic X-mode at 82.7 GHz. In addition, the heating beam with 1 MW of neutral power has been available which injects deuterium atoms tangentially with a full energy of 25 keV. The geometry of the NBI source and an orbit of a corresponding 25 keV ion with a pitch value ($p = v_{||}/v$) of 0.9 are plotted in figure 1. The Fast-Ion D-Alpha (FIDA [2]) technique has been employed at TCV to study the fast-ion distribution function experimentally. FIDA spectroscopy is a charge-exchange recombination spectroscopy (CXRS) method that makes use of the charge exchange reaction between donor neutrals (such as the injected beam neutrals, beam halo neutrals or background neutrals) and the fast ions. The resulting fast neutrals emit Balmer alpha radiation which can be observed with large Doppler shifts. Depending on the observation geometry and Doppler shift, different parts of the fast-ion velocity space are probed. At TCV two observation geometries are available which are shown in blue in figure 1. Firstly, an array of toroidal lines of sight (toroidal view) is used which originally belongs to the CXRS system[3] and intersects a diagnostic beam (DNB) [4]. Secondly, a new optical system has been installed which observes the heating beam from the top (poloidal view). The
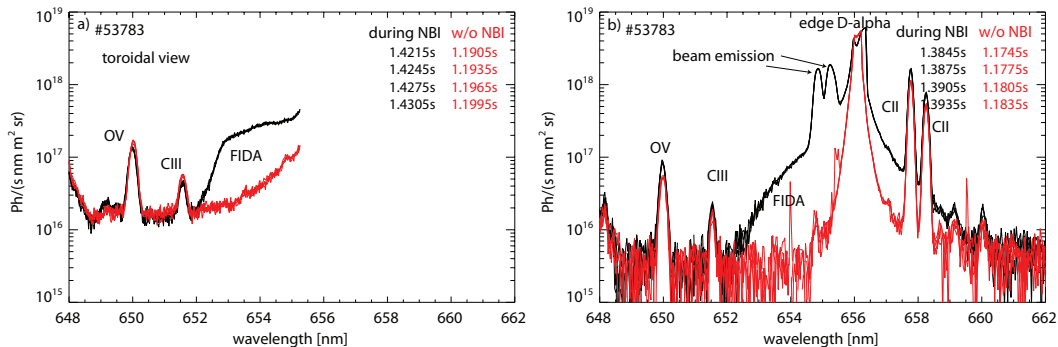
FIG. 2: *Measured spectra with a toroidal (a) and poloidal (b) line of sight without (red) and during operation of the heating beam (black).*

toroidal view is sensitive to co-rotating fast ions while the poloidal view is more sensitive to fast ions with small pitch values. Measured spectra for one representative channel of each system are shown in figure 2. As can be seen, the toroidal system is set up to observe only up to 655 nm which avoids the unshifted D-alpha line at 656.1 nm. The latter is intense in the toroidal observation and would cause strong saturation effects. The poloidal view, instead, observes the whole D-alpha spectrum with only modest saturation of the detector at 656.1 nm. This is possible because less unshifted D-alpha light is observed along the lines of sight. The latter have a shorter intersection with the plasma (80 cm instead of 130 cm) and are less tangential to the plasma edge than the toroidal lines of sight. The spectra in red in figure 2 have been measured without NBI while those in black have been acquired when NBI was on. The broad spectral component of the FIDA light is only present during NBI. Interestingly, the DNB was off during the acquisition of the toroidal spectrum (figure 2a). This shows that this FIDA radiation is of passive nature and originates from charge exchange reactions between background neutrals and fast ions. In contrast, the poloidal measurement is dominated by active radiation since the heating beam causes intense charge exchange emissions. The poloidal measurement also exhibits two peaks of the beam emission (full and half energy component) near 655 nm which can be used to calibrate the measurement.

Analysis of NBI experiments

Several experiments with an upwards shifted (10 cm) plasma have been performed which feature slight off-axis NBI injection. The discharges have been conducted in limiter configuration with a clockwise directed magnetic field of 1.43 T and a clockwise directed current of 180 kA. This provides co-injection from the NBI and hence small first orbit losses. Figure 3a shows time traces of a representative discharge (#53778). The discharge was heated by 0.5 MW of central ECRH which was additionally used to drive a counter current. This allowed us to avoid sawtooth crashes which would affect the fast-ion distribution function otherwise. Between 1.2 s and 1.7 s the heating beam was turned on with 0.9 MW of power (assuming 100 kW of neutral beam losses in the beam duct), which
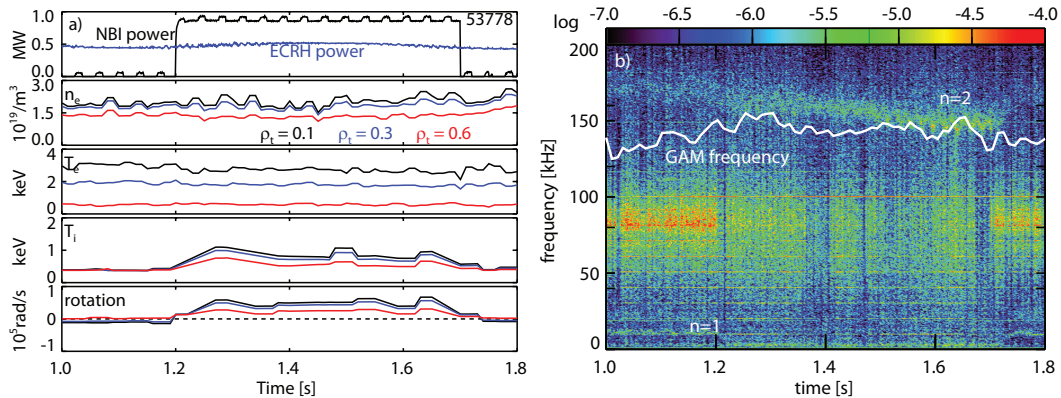
FIG. 3: *a) Representative time traces of discharge #53778 (off-axis) b) Magnetic spectrogram for discharge #53778 (off-axis). The estimated GAM frequency is plotted in white.*

increases the central ion temperature ($T_i(0) = 0.4$ keV $\rightarrow$ 1.0 keV) and toroidal plasma rotation frequency ($f_{tor}(0) = $ -10 krad/s $\rightarrow$ 60 krad/s). The electron temperature remains unaffected during the application of NBI because ion heating dominates at high electron temperatures [5]. Figure 3b shows a magnetic spectrogram. Only very weak magnetohydrodynamic (MHD) activity with a toroidal mode number of $n = 1$ has been identified at 10 kHz which disappears during the application of NBI. In the frequency band between 50 kHz and 100 kHz, machine related perturbations appear which are also visible after plasma discharges. At higher frequencies, a $n = 2$ mode becomes visible during the NBI phase that might be explained by beta induced Alfvén eigenmodes (BAEs) [6]. BAEs appear at the geodesic acoustic mode (GAM) frequency which has been estimated for core localized modes using the TRANSP equilibrium and kinetic profiles. As can be seen in 3b, the estimated GAM frequency is close to the MHD activity at 150 kHz. The modes are well known to appear when the electron temperature is significantly larger than the ion temperature and can be excited by 25 keV fast ions since these exhibit a toroidal orbit frequency of 280 kHz. TRANSP [7] simulations have been performed to model the experiment using kinetic profiles from the Thomson and CXRS diagnostics. The effective charge profile is assumed constant over the radius and time and is determined by matching predicted and measured loop voltages during ohmic plasma conditions (Z_{eff}=3). Moreover, different ion particle confinement times (τ_i) were assumed which determine the background neutral density, calculated by the FRANTIC module (a part of TRANSP). The 1D model FRANTIC can describe the penetration of neutrals from the walls into the plasma. By assuming a value for τ_i and considering the ion density profile, FRANTIC determines the radial ion outflow which must be balanced by the ionization of background neutrals. The predicted evolution of the contributions to the plasma current are plotted in figure 4a for $\tau_i = 5$ ms (a neutral density at the plasma boundary of 2×10^{10}/cm^3). While the bootstrap current and ECCD remain constant throughout the displayed time window, the fast-ion current is about 40 kA after turning on NBI heating. During the
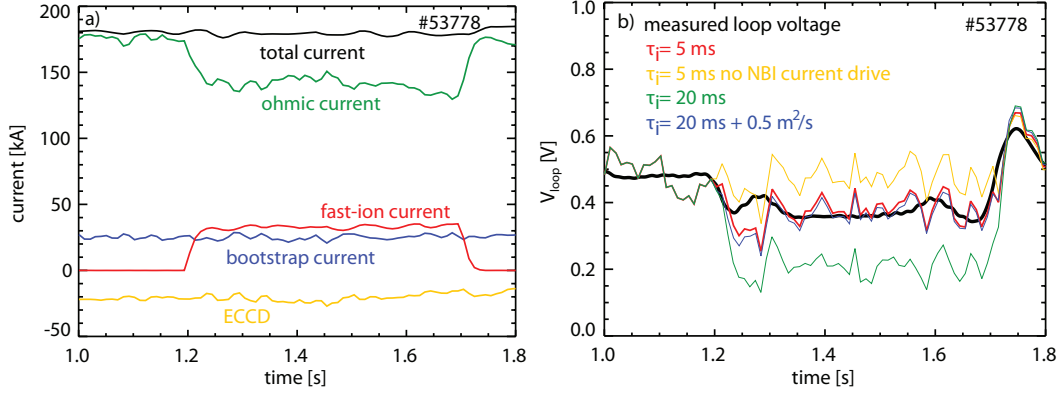
FIG. 4:   a) TRANSP predicted temporal evolution of the contributions to the plasma
current. b) Measured (black, smoothed by a low-pass filter) and predicted loop voltage.
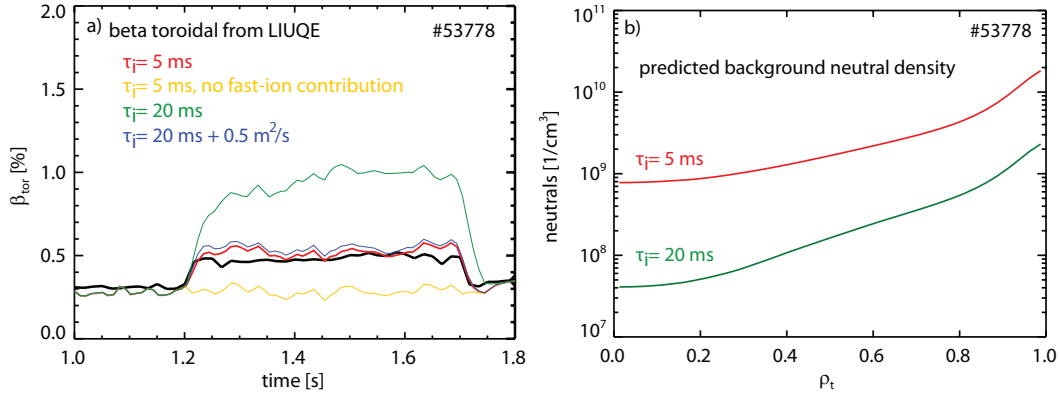

FIG. 5:   a) Measured and predicted toroidal beta. b) Predicted radial density profile of
neutrals at 1.39 s.

NBI phase, the ohmic current that is necessary to maintain the total plasma current is
reduced accordingly. This reduction of the ohmic current can be observed experimentally
by a reduction of the loop voltage, plotted in figure 4b. The reduction of the measured
loop voltage during NBI is in good agreement with the TRANSP predicted loop voltage
for $\tau_i = 5$ ms and considering the fast-ion contribution to the current. When instead
setting the fast-ion current to zero in the simulation, the predicted loop voltages (shown
in yellow) do not drop during the NBI phase. This proves that the fast-ion current drive
is effective at TCV and that the drop is not an artifact of the change in kinetic profiles.
A similar behavior can be seen in the measured toroidal beta value, i.e. the plasma pres-
sure divided by the pressure of the toroidal magnetic field. As plotted in figure 5a, the
toroidal beta, determined by the equilibrium reconstruction, increases when switching on
NBI. This increase is well described by the TRANSP simulation for $\tau_i = 5$ ms with the
fast-ion contribution to the total pressure. When instead only considering a predicted
beta without the fast-ion contribution, no increase is expected (yellow simulation). Fig-
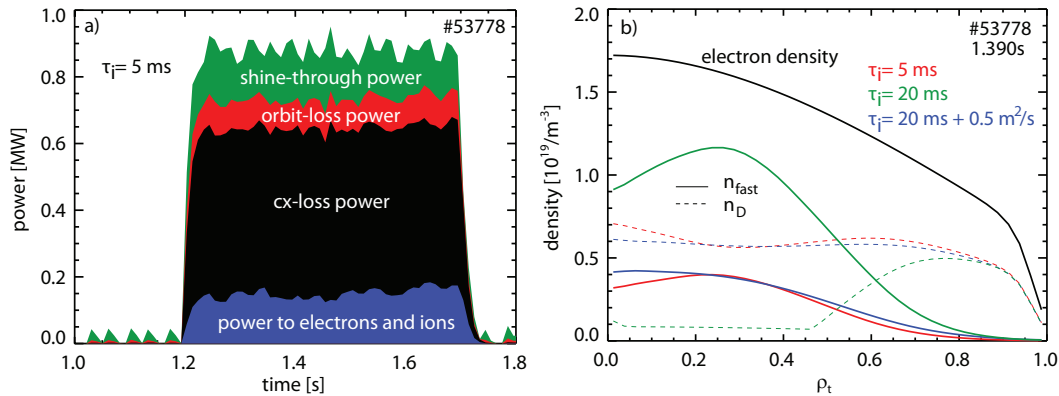
FIG. 6: a) TRANSP predicted losses and the power to electrons and ions (blue) when assuming $\tau_i = 5$ ms. b) Predicted radial fast-ion and deuterium ion density profiles.

ure 5b shows the radial profile of neutrals from TRANSP. Large neutral densities are predicted when assuming $\tau_i = 5$ ms which cause strong charge exchange losses of up to 500 kW, as illustrated in figure 6a. By additionally considering orbit losses (about 100 kW) and shine through losses (about 200 kW), the remaining heating power of ions and electrons is reduced to less than 150 kW. To check this significant difference between applied and coupled NBI heating power (only 15% reaches the plasma) we compare the thermal stored energy w_{th} based on the kinetic profiles with the Kaye L-mode scaling [8] where $w_{th} \propto P^{0.27}$ is expected. The scaling, combined with the low beam heating predicted by TRANSP roughly agrees with the measured stored energy (the scaling predicts 10-20% larger stored energies). This confirms the reduced fast-ion density needed to match the measured and predicted values of the loop voltage and toroidal beta. The origin of the reduced heating efficiency can be fully explained by charge exchange losses on neutrals. However, $\tau_i = 5$ ms is an undiagnosed free parameter which we chose to obtain a good match between simulated and experimental data. To illustrate the sensitivity of the fast-ion density to τ_i, simulated radial fast-ion density profiles are shown in figure 6b for $\tau_i = 5$ ms and $\tau_i = 20$ ms. As can be seen, the fast-ion density is significantly larger for $\tau_i = 20$ ms. It should be noted that simulations with even larger τ_i values (e.g. 30 ms) are not possible in TRANSP because the fast-ion density would exceed the deuterium ion density (shown in figure 6b by the dashed lines). Results of the simulation assuming $\tau_i = 20$ ms have already been plotted in green in figures 4b and 5a. As can be seen, the assumption of weak charge exchange losses and, thus, large fast-ion densities does not agree with the experimental data. Figure 7a compares active FIDA spectra (the background radiation has been subtracted) with predictions from FIDASIM [9] (active + passive radiation) that are based on TRANSP predicted fast-ion distribution functions. The measurement has been scaled to match the predicted beam emission. The simulation plotted in red corresponds to the neoclassical simulation assuming $\tau_i = 5$ ms and shows good agreement with the measured shape. In contrast, the neoclassical sim-
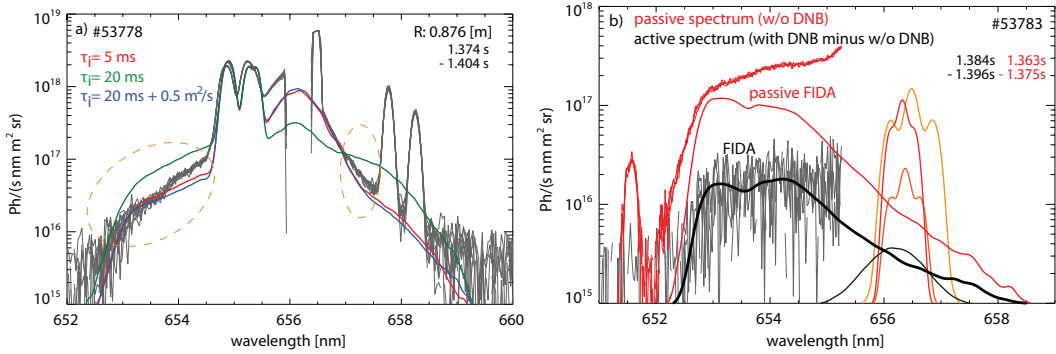
FIG. 7: a) Active poloidal FIDA spectrum and predictions from FIDASIM. The ovals in orange indicate the regions of interest for the interpretation of the spectra. b) Active and passive toroidal FIDA spectrum compared with predictions from FIDASIM.

ulation assuming $\tau_i = 20$ ms in green clearly overestimates the measurement and thus confirms analysis of the loop voltage and toroidal beta. However, good agreement with the experimental data can also be obtained when adding anomalous fast-ion transport to the simulation. When e.g. considering $\tau_i = 20$ ms and a constant ad hoc diffusion of fast ions of $0.5 m^2/s$ (comparable with values used e.g. in [10]), the corresponding synthetic FIDA spectrum shown in blue agrees with the data. The simulation is also consistent with the measured loop voltage and beta toroidal, shown in blue in figures 4b and 5a. This indicates that large charge exchange losses are not the only explanation for the low coupled NBI power. Anomalous transport could be responsible as well. However, from passive FIDA measurements by the toroidal view, it is clear that there is a significant density of background neutrals. Figure 7b compares an active spectrum from the toroidal view with the simulation for a similar discharge (#53783). The data (black) has been scaled such that it coincides with the predicted active FIDA component. In addition, the passive radiation is plotted in red which is much stronger than the active radiation. The large passive signal can be reproduced by FIDASIM when considering the neutral density from TRANSP ($\tau_i = 5$ ms). In addition, absolutely calibrated measurements of the compact neutral particle analyzer (CNPA[11]) agree with the assumption of $\tau_i = 5$ ms. This suggests that the predicted neutral density is of the right order of magnitude. The simulation without anomalous diffusion might therefore be an appropriate representation of the experiments at TCV. However, it should be noted that the neutral density considered by TRANSP and FIDASIM is poloidally symmetric which is typically not the case in tokamak plasmas. Moreover, FIDASIM does not consider fast ions outside the boundary which neglects possible passive FIDA radiation from outside the plasma. These two effects could increase the predicted passive FIDA radiation.

Conclusion and Outlook

Experiments with 1 MW of nominal NBI power (25 keV, deuterium) have been performed that feature very low electron densities and high electron temperatures. The

TRANSP code has been applied to simulate the fast-ion slowing down distribution and to compare predicted loop voltages and toroidal beta values with the measurements. Hereby, best agreement is obtained when considering strong fast-ion losses such that only 15% of the nominal beam power is coupled to the plasma. The fast-ion losses are even necessary for the TRANSP simulations becuse otherwise, the fast-ion density would overcome the total deuterium ion density. The observed weak modification of the kinetic profiles also agrees with the Kaye L-mode scaling when considering the low NBI heating efficiency. In addition, synthetic spectra from FIDASIM which represent the TRANSP prediction match active FIDA measurements from a poloidal view. A reduction of the predicted fast-ion density can be obtained by assuming anomalous fast-ion transport in the TRANSP simulations. Furthermore, strongly reduced fast-ion densities also obtained when considering charge exchange losses due to background neutrals. The presence of large neutral densities is supported by passive FIDA signals from toroidal lines of sight and by neutral fluxes measured with the absolutely calibrated compact neutral particle analyzer. This shows that charge exchange losses have a significant effect on the fast-ion density and NBI heating efficiency at TCV when the electron denisty is very low. The fast-ion redistribution induced by high frequency MHD activity, as observed during NBI heating and attributed to beta induced Alfvén eigenmodes, is therefore difficult to quantify. The impact of charge exchange losses cannot be characterized accurately enough to draw clear conclusions on the level of anomalous fast-ion transport. More detailed investigations of the neutral density are thus necessary for future studies.

References

[1] KARPUSHOV, A. N. et al., Fusion Engineering and Design **9697** (2015) 493.

[2] GEIGER, B. et al., Plasma Physics and Controlled Fusion **53** (2011) 065010.

[3] DUVAL, B. P. et al., Physics of Plasmas **15** (2008) 056113.

[4] KARPUSHOV, A. N. et al., Fusion Engineering and Design **84** (2009) 993.

[5] STIX, T. H., Plasma Physics **14** (1972) 367.

[6] CHEN, W. et al., Physics Letters A **377** (2013) 387.

[7] HAWRYLUK, R. et al., in Physics of Plasmas Close to Thermonuclear Conditions **1** (1980) 19.

[8] KAYE, S. et al., Nuclear Fusion **37** (1997) 1303.

[9] HEIDBRINK, W. et al., Commun. Comput. Phys. **10** (2011) 716.

[10] GEIGER, B. et al., Plasma Physics and Controlled Fusion **57** (2015) 014018.

[11] KARPUSHOV, A. N. et al., Review of Scientific Instruments **77** (2006) 033504.